Candida albicans transcription factor Rim101 mediates pathogenic interactions through cell wall functions

Nobile, Clarissa J.; Solis, Norma; Myers, Carter L.; Fay, Allison J.; Deneault, Jean-Sebastien; Nantel, Andre; Mitchell, Aaron P.; Filler, Scott G.

Publisher's version / Version de l'éditeur:
https://doi.org/10.1111/j.1462-5852.2008.01198.x
Cellular Microbiology, 10, 11, pp. 2180-2196, 2008-07-23

Published in final edited form as:
Cell Microbiol. 2008 November ; 10(11): 2180–2196. doi:10.1111/j.1462-5822.2008.01198.x.

Candida albicans transcription factor Rim101 mediates pathogenic interactions through cell wall functions

Clarissa J. Nobile[1], **Norma Solis**[2], **Carter L. Myers**[2], **Allison J. Fay**[1], **Jean-Sebastien Deneault**[3], **Andre Nantel**[3], **Aaron P. Mitchell**[1,5], and **Scott G. Filler**[2,4]

1*Department of Microbiology, Columbia University, New York, NY, USA*

2*Los Angeles Biomedical Research Institute at Harbor-UCLA Medical Center, Torrance, CA, USA*

3*Biotechnology Research Institute, National Research Council of Canada, Montreal, PQ, Canada*

4*David Geffen School of Medicine at UCLA, Los Angeles, CA, USA*

Abstract

pH-responsive transcription factors of the Rim101/PacC family govern virulence in many fungal pathogens. These family members control expression of target genes with diverse functions in growth, morphology, and environmental adaptation, so the mechanistic relationship between Rim101/PacC and infection is unclear. We have focused on Rim101 from *Candida albicans*, which we find to be required for virulence in an oropharyngeal candidiasis (OPC) model. Rim101 affects the yeast-hyphal morphological transition, a major virulence requirement in disseminated infection models. However, virulence in the OPC model is independent of the yeast-hyphal transition because it is unaffected by an *nrg1* mutation, which prevents formation of yeast cells. Here we have identified Rim101 target genes in an *nrg1Δ/Δ* mutant background and surveyed function using an overexpression-rescue approach. Increased expression of Rim101 target genes *ALS3, CHT2, PGA7/RBT6, SKN1*, or *ZRT1* can partially restore pathogenic interaction of a *rim101Δ/Δ* mutant with oral epithelial cells. Four of these five genes govern cell wall structure. Our results indicate that Rim101-dependent cell wall alteration contributes to *C. albicans* pathogenic interactions with oral epithelial cells, independently of cell morphology.

INTRODUCTION

Candida albicans is the major invasive fungal pathogen of humans, with the capacity to cause both disseminated and mucosal infection. Distinct risk factors govern susceptibility to each type of infection (Enoch *et al*., 2006, Edmond *et al*., 1999). Hence, it is probable that different attributes of *C. albicans* may be critical for virulence in each type of infection. Numerous fungal genes and regulatory pathways that contribute to the capacity of *C. albicans* to cause disseminated infections have been defined through mutant analysis with animal models and, increasingly, with in vitro cell or tissue interaction systems (Ramirez *et al*., 2007, MacCallum *et al*., 2006, Schaller *et al*., 2005, Calera *et al*., 1999). Much less is known about the fungal determinants required for mucosal infection.

Our focus here is oropharyngeal candidiasis (OPC), a candidal infection of the oral mucosa. We have recently employed in vitro epithelial cell interaction assays to identify steps in host cell-pathogen interaction that may be critical for establishment of OPC. These steps include

Address correspondence to: Aaron P. Mitchell (E-mail: apm1@andrew.cmu.edu) and Scott G. Filler (E-mail: sfiller@ucla.edu)..
[5]Current address for A.P. Mitchell: Department of Biological Sciences, Carnegie Mellon University, Pittsburgh, PA 15213

the binding of *C. albicans* to oral epithelial cells, endocytosis of *C. albicans*, and the resulting loss of epithelial cell integrity, or damage (Park *et al*., 2005). The overall ability to cause epithelial cell damage in vitro has served empirically as a predictor of the capacity of *C. albicans* strains to cause OPC in an immunosuppressed mouse infection model. Such analysis led to our finding that the *C. albicans* protein kinases Tpk2 and Cka2 are required for virulence during OPC (Chiang *et al*., 2007, Park *et al*., 2005). Interestingly, Tpk2 and Cka2 have minor roles in virulence during hematogenously disseminated candidiasis (Chiang *et al*., 2007, Park *et al*., 2005). These findings support the significance of the in vitro epithelial cell interaction assays and illustrate that distinct *C. albicans* genes govern virulence in the context of OPC.

Among the major regulators of the capacity of *C. albicans* to cause disease during a disseminated infection are the transcription factors Rim101 and Nrg1 (Davis *et al*., 2000a, Saville *et al*., 2003). Rim101 is a member of the Rim101/PacC family of C_2H_2 zinc finger transcription factors that govern gene expression responses to extracellular pH (Penalva *et al*., 2004). Rim101/PacC family members have diverse roles in virulence of fungal pathogens. In mice, *C. albicans* Rim101 and *Aspergillus nidulans* PacC are required for virulence during disseminated candidiasis and invasive pulmonary aspergillosis, respectively (Davis *et al*., 2000a, Bignell *et al*., 2005). In plants, *Sclerotinia sclerotiorum* Pac1 and *Colletotrichum acutatum* Klap2, a Rim101 homolog, are required for pathogenicity (Rollins, 2003, You *et al*., 2007). However, *Ustilago maydis* Rim101 has no detectable role in plant infection, and *Fusarium oxysporum* PacC functions as a negative regulator of virulence in plant infection (Arechiga-Carvajal *et al*., 2005, Caracuel *et al*., 2003). Thus the precise roles of Rim101/PacC family members in infection vary significantly.

Nrg1 is also a C_2H_2 zinc finger transcription factor. *C. albicans* Nrg1 is a negative regulator of hyphal formation under in vitro and in vivo growth conditions (Braun *et al*., 2001, Murad *et al*., 2001, Saville *et al*., 2003). The ability to form hyphae is a critical *C. albicans* pathogenicity trait in disseminated infection models (Saville *et al*., 2003, Lo *et al*., 1997), so one might expect an *nrg1Δ/Δ* mutant to be hypervirulent. However, the mutant is attenuated in a disseminated infection model (Murad *et al*., 2001). These findings suggest that the capacity to produce yeast form cells, as well as hyphae, is required for disseminated infection. In fact, a recent study showed that although hyphae are required for the mortality of a *C. albicans* infection, it is the yeast form cells that are most important for disseminating the infection (Saville *et al*., 2003).

In one context, Rim101 and Nrg1 have opposite functions: Rim101 promotes hyphal formation in response to neutral or alkaline growth conditions; Nrg1 inhibits hyphal formation under all conditions. In keeping with these observations, of seven hyphal-specific genes that are under positive control by Rim101, four are also under negative control by Nrg1 (Bensen *et al*., 2004). However, Bensen et al. have argued that Rim101 and Nrg1 act in parallel hyphal regulatory pathways (Bensen *et al*., 2004). This inference was based on the finding that *C. albicans* Rim101 does not repress *NRG1* expression, in contrast to the situation in *S. cerevisiae* (Lamb *et al*., 2003). In addition, a *rim101Δ/Δ nrg1Δ/Δ* double mutant was slightly less filamentous than an *nrg1Δ/Δ* single mutant in M199 medium at pH 8. The existence of Rim101 targets that are independent of Nrg1 is substantiated by microarray analysis (Bensen *et al*., 2004). For example, of ten cell wall genes that are under positive control by Rim101, only one is under negative control by Nrg1. Examination of Rim101 targets that are independent of Nrg1 may yield mechanistic insight into Rim101 functions that are independent of hyphal formation.

In this study, we examine the relationship between Rim101 and Nrg1 in OPC infection models. Our results indicate that the role of Rim101 in the pathogenesis of OPC is independent of Nrg1, thus prompting a focus on Rim101 target genes that are independent of Nrg1. Our findings

point to the cell surface as a major mediator of the role of Rim101 in pathogenicity during OPC.

RESULTS

RIM101 Governs the Capacity of C. albicans to Damage Oral Epithelial Cells Independently of NRG1

Rim101 and Nrg1 are each required for virulence of *C. albicans* in disseminated infection models (Davis *et al*., 2000a, Saville *et al*., 2003, Braun *et al*., 2001, Murad *et al*., 2001). To determine whether they may also have roles in virulence during OPC, we investigated the capacity of single and double mutant strains to damage the FaDu oral epithelial cell line (Figure 1A), a trait that is correlated with virulence in a mouse OPC model (Park *et al*., 2005, Chiang *et al*., 2007). The *rim101*Δ/Δ mutant caused little epithelial cell damage compared to either the wild-type or *rim101*Δ/Δ + p*RIM101* complemented strain. In contrast, the *nrg1*Δ/Δ mutant caused similar levels of epithelial cell damage to the wild-type and complemented strains. To investigate potential interactions of *RIM101* and *NRG1*, we measured the extent of epithelial cell damage induced by a *rim101*Δ/Δ *nrg1*Δ/Δ double mutant. This strain caused almost no detectable damage to the epithelial cells (Figure 1B). Complementing this mutant with a wild-type copy of *RIM101*, but not *NRG1*, restored its capacity to damage epithelial cells to same level as the wild-type strain. These results indicate that *RIM101* is required, independently of *NRG1*, for *C. albicans* to damage oral epithelial cells in vitro.

Effects of RIM101 and NRG1 on C. albicans Morphology

In several in vitro infection models, host cell damage capacity correlates with *C. albicans* morphology (Phan *et al*., 2000, Park *et al*., 2005, Villar *et al*., 2004). Thus we examined the morphology of each strain after a 3-hour incubation on oral epithelial cells. As expected, the wild-type strain formed true hyphae on these cells (Figure 2A) (Park *et al*., 2005, Chiang *et al*., 2007). The *rim101*Δ/Δ strain formed a mixture of true hyphae and pseudohyphae that were slightly shorter than those of the wild-type strain (Figure 2B). As expected, the *nrg1*Δ/Δ strain grew as pseudohyphae even under normally non-hyphal inducing conditions (data not shown). On the epithelial cells, the pseudohyphae of this strain were considerably longer and contained more branches than the true hyphae of the wild-type strain (Figure 2C). The *rim101*Δ/Δ *nrg1*Δ/Δ double mutant formed pseudohyphae that were highly branched and slightly shorter than those of the *nrg1*Δ/Δ mutant, but longer than the hyphae of the wild-type strain (Figure 2D). Complementation of each single mutant restored the wild-type phenotype (Figure 2E, 2H). Also, introduction of a wild-type *RIM101* allele into the *rim101*Δ/Δ *nrg1*Δ/Δ double mutant produced a phenotype similar that of the *nrg1*Δ/Δ mutant (Figure 2G); introduction of a wild-type *NRG1* allele into the *rim101*Δ/Δ *nrg1*Δ/Δ double mutant yielded a phenotype similar that of the *rim101*Δ/Δ mutant (Figure 2F). Thus it is possible that the altered morphology of the *rim101*Δ/Δ strain may contribute to its host damage defect. However, the finding that pseudohyphae of the *nrg1*Δ/Δ single mutant damaged epithelial cells, whereas pseudohyphae of the *rim101*Δ/Δ *nrg1*Δ/Δ double mutant did not suggests that *RIM101* is required for host cell damage independently of its role in cell morphology.

RIM101 is Required for C. albicans to Invade Oral Epithelial Cells

C. albicans invades oral epithelial cells in vitro by inducing its own endocytosis (Drago *et al*., 2000, Park *et al*., 2005, Chiang *et al*., 2007), and cell damage is closely associated with the endocytosis of live organisms (Park *et al*., 2005). Therefore, we investigated whether *RIM101* is required for epithelial cell damage because it is required to induce endocytosis. These experiments were performed using the *rim101*Δ/Δ *nrg1*Δ/Δ double mutant and two complemented strains (a *rim101*Δ/Δ *nrg1*Δ/Δ + p*RIM101* strain and a *rim101*Δ/Δ *nrg1*Δ/Δ + p*NRG1* strain). Significantly fewer cells of the *rim101*Δ/Δ *nrg1*Δ/Δ double mutant were

endocytosed by the epithelial cells compared to those of the wild-type strain (Figure 3A). Introduction of a wild-type copy of *RIM101*, but not *NRG1*, into the *rim101*Δ/Δ *nrg1*Δ/Δ double mutant increased its capacity to induce endocytosis to greater than the wild-type levels. Therefore, *RIM101* is necessary for *C. albicans* to induce maximal endocytosis by oral epithelial cells. Furthermore, *NRG1* is a negative regulator of *C. albicans* invasion of epithelial cells.

We also measured the number of organisms that were associated with the epithelial cells, which was defined as the sum of the adherent and endocytosed organisms (Figure 3B). Over 2-fold more cells of the *rim101*Δ/Δ *nrg1*Δ/Δ double mutant were cell-associated compared to the wild-type strain, despite the finding that the double mutant is defective in inducing endocytosis. Introduction of either *RIM101* or *NRG1* wild-type alleles caused significant reduction in cell association. However, the number of cell-associated organisms of either complemented strain was still greater than that of the wild-type strain (Figure 3B). These observations indicate that both *RIM101* and *NRG1* are negative regulators of *C. albicans* adherence, and that and adherence defect is not the cause of the *rim101*Δ/Δ-associated endocytosis defect.

RIM101 is necessary for maximal virulence during OPC

The virulence of the *rim101*Δ/Δ *nrg1*Δ/Δ double mutant and its two complemented strains was tested in a mouse model of OPC. Mice infected with the *rim101*Δ/Δ *nrg1*Δ/Δ double mutant had significantly lower oral fungal burden than did mice infected with the wild-type strain (Figure 4). Complementing this double mutant with a wild-type copy of *RIM101* restored its virulence to that of the wild-type strain. However, complementing the double mutant with a wild-type allele of *NRG1* did not increase its virulence. These results indicate that *RIM101* is required for virulence in this model.

The relative extent of oropharyngeal disease in mice infected with the various strains was also assessed by histopathologic examination. Mice infected with the wild-type strain had large oral lesions containing extensive fungal elements (Figure 5A). In contrast, mice infected with the *rim101*Δ/Δ *nrg1*Δ/Δ double mutant had much smaller oral lesions that contained proportionally fewer organisms (Figure 5B), in agreement with our quantitative fungal burden determinations (Figure 4). Complementation with *RIM101* resulted in large oral lesions that were similar to those induced by the wild-type strain (Figure 5C), whereas complementation with *NRG1* resulted in lesions that resembled those induced by the *rim101*Δ/Δ *nrg1*Δ/Δ double mutant (Figure 5D). These results indicate that *RIM101*, but not *NRG1*, is essential for maximal virulence during OPC.

Identification of Nrg1-Independent Rim101 Target Genes

We used microarray analysis to identify Rim101 target genes that may mediate virulence in the OPC model. Specifically, we identified Rim101-dependent genes in an *nrg1*Δ/Δ mutant background by comparing gene expression profiles of the *rim101*Δ/Δ *nrg1*Δ/Δ double mutant and the *rim101*Δ/Δ *nrg1*Δ/Δ + p*RIM101* complemented strain (Supplemental data, “All genes” worksheet). We found 366 genes whose expression levels varied more than 1.5-fold between these strains (Supplemental data, “Rim101 regulated” worksheet). Rim101-dependent expression of several genes was verified by independent methods (Supplemental Figure 1). Thirty six of these genes were identified as Rim101-responsive in a previous comparison in an *NRG1* background (Bensen *et al*., 2004) (Supplemental data, “Shared Rim101 regulated” worksheet). We identified many additional Rim101-responsive genes (Supplemental data, “New Rim101 regulated” worksheet), including *SAP5, SOD5, CHT2, ALS3, CSA2*, and *SKN1*. Many of these new genes extend known Rim101-regulated gene categories (Bensen *et al*., 2004), with functional connections to the cell wall, transport, and amino acid synthesis (see examples in Table 2).

Functional Analysis of Rim101-Dependent Genes

We considered the hypothesis that Rim101 promotes virulence through activation of specific target genes. To test this hypothesis, we overexpressed individual Rim101-dependent genes by fusion to the strong *TDH3* promoter in a *rim101*Δ/Δ mutant. We chose nine of the most highly Rim101-dependent genes, including *CFL2/FRE2, CHT2*, *CSA1, ECE1, FAA2, PGA7/RBT6, SAP5, SKN1*, and *ZRT1*. We also chose *ALS3*, because we had observed that Rim101 is required for N-cadherin binding to *C. albicans*(Phan, Filler, and Mitchell, unpublished data), a known function of Als3 (Phan *et al*., 2007). Increased expression of each gene was verified by RTPCR or flow cytometry (Supplemental Figures 2 and 3). We tested each target gene overexpressing (TGO) strain for characteristic *rim101*Δ/Δ mutant phenotypes, including lack of growth on YPD medium containing LiCl, lack of growth on YPD pH 9.0 medium, and lack of filamentation on M199 pH 8.2 medium. All TGO strains behaved similarly to the *rim101*Δ/Δ mutant in these assays (data not shown). Therefore, no single target gene tested is responsible for these in vitro phenotypes.

We also tested each TGO strain in the damage and endocytosis assays; positive results were replicated with an independent TGO isolate. Overexpression of *ECE1*, *CSA1, SAP5*, or *CFL2/FRE2* had no effect on the *rim101Δ/Δ* defects (data not shown). However, overexpression of *ALS3, CHT2*, or *SKN1* in the *rim101Δ/Δ* background resulted in greater epithelial cell damage (Figure 6A). In addition, overexpression of *ALS3, CHT2, PGA7/RBT6*, or *ZRT1* consistently caused increased endocytosis by epithelial cells (Figure 7). These results argue that *ALS3, CHT2, PGA7/RBT6, SKN1*, and *ZRT1* contribute to the Rim101-dependent pathogenic interactions with epithelial cells.

There is growing evidence that cell wall perturbation may have complex effects on fungal pathogens that result in hypervirulence (Kamran *et al*., 2004, MacCallum *et al*., 2006, Wheeler *et al*., 2006). We considered this explanation for our results because several of the functional Rim101 target genes affect the cell surface. Thus we investigated whether overexpression of these Rim101 target genes in the wild-type strain influenced the extent of epithelial cell damage. Increased expression of *CHT2*and *SKN1* in DAY185 caused a 3% and 5% increase in epithelial cell damage, respectively (Figure 6B). The magnitude of this increase in damage was much less than occurred when these genes were overexpressed in the *rim101Δ/Δ* mutant. Furthermore, overexpression of *ALS3* in the wild-type strain had no effect on epithelial cell damage, even though overexpression of this gene in the *rim101Δ/Δ* mutant resulted in a significant increase in damage. Collectively, these results support the model that reduced epithelial cell damage caused by the *rim101Δ/Δ* mutant is due in part to its reduced expression of *ALS3, CHT2*, and *SKN1*.

DISCUSSION

Analysis of Transcription Factors to Understand Virulence Mechanisms

Transcription factors have been viewed with both delight and disdain for their potential in elucidating the mechanistic basis of such complex traits as pathogenicity. In the study of *C. albicans*, this dichotomy came to the foreground with studies of Efg1 and Cph1. These transcription factors are required for both hyphal formation and pathogenicity, thus linking cell morphogenesis to virulence (Lo *et al*., 1997, Phan *et al*., 2000). However, the more skeptical view was that transcription factors are expected to have multiple target genes, and some Efg1/Cph1 targets might be required for pathogenicity independently of any cellular morphogenetic feature. Indeed, subsequent studies have shown that several Efg1/Cph1-dependent genes that are required for virulence are not required for hyphal morphogenesis (Staib *et al*., 2002, Felk *et al*., 2002, Korting *et al*., 2003, Lane *et al*., 2001). On the other hand, the utility of studying

Efg1 and Cph1 has also been illustrated by these subsequent studies, precisely because so many Efg1/Cph1 target genes have roles in virulence.

Our current study of Rim101 and Nrg1 illustrates some useful features of a focus on transcription factors. First, because Rim101 is required for pathogenicity in the OPC model and Nrg1 is not, we could concentrate on Rim101 target genes in an *nrg1Δ/Δ* mutant background, thus avoiding a focus on morphogenesis-related genes. In addition, our approach may have circumvented genetic redundancy. For gene families, deletion of several family members may be necessary to cause an altered phenotype. Many Rim101 target genes are in gene families, including *ALS, SAP, FRE/CFL, CHT*, and *RBT5*-related genes. The phenotypic impact of overexpressed genes may have resulted from the fact that Rim101 is required for expression of several members of each gene family. In terms of pathogenicity, analysis of these transcription factor mutants has led to new connections between target genes and phenotype.

Role of Nrg1 in OPC

Nrg1 is required for virulence in a disseminated infection model, a fact established with two independent *nrg1*Δ/Δ strains in two different labs (Murad *et al*., 2001, Braun *et al*., 2001). The constitutive pseudohyphal formation is likely a major factor in the reduced virulence of *nrg1*Δ/Δ strains when they are inoculated into mice via the tail vein. The *nrg1*Δ/Δ pseudohyphae probably lodge in the pulmonary capillaries where they are killed by the resident macrophages before they can be carried by the blood to the kidney, the usual target organ in mice with hematogenously disseminated candidiasis. Aberrant trafficking of the *nrg1*Δ/Δ strain did not occur in our model of OPC because all strains were applied directly to the oral mucosa. We assayed virulence through both fungal burden and histopathology, which gave consistent results. This finding correlated well with our discovery that an *nrg1*Δ/Δ strain had no defect in damaging an oral epithelial cell line. Thus far, only one other gene, *IRS4*, is required for disseminated candidiasis but not OPC (Badrane *et al*., 2005).

Two genes, *CKA2* and *TPK2*, are required for virulence during OPC but not disseminated candidiasis, the converse of *NRG1* (Chiang *et al*., 2007, Park *et al*., 2005). There are numerous differences between the infection sites in these two diseases, so it seems reasonable to expect genes of these two classes. In the disseminated candidiasis model, mutants locked in either the yeast or filamentous growth forms are attenuated (Navarro-Garcia *et al*., 2001). This finding indicates that conversion between the forms is required for virulence in the disseminated infection model. In the OPC model, the nonfilamentous *efg1*Δ/Δ mutant is attenuated (Park *et al*., 2005), thus arguing that filamentous growth forms are required for OPC. However, our findings with the hyperfilamentous *nrg1Δ/Δ* mutant suggest that the yeast growth form is not required for virulence in the OPC model.

Identification of New Rim101-Dependent Genes

Many of the most highly regulated Rim101-dependent genes in our data set are hyphal-specific genes, including *SOD5, CSA2, PGA7/RBT6, ECE1, CSA1, SAP5, HYR1*, and *RBT5*. This result is consistent with the previous finding that Rim101 is required for hyphal-specific gene expression (Bensen *et al*., 2004). Our microarray results also demonstrate that Rim101 governs expression of at least some of these genes independently of Nrg1, in keeping with prior studies (Liu, 2001, Bensen *et al*., 2004).

Our data identified 175 new Rim101-dependent genes. Ninety-one new genes may be direct Rim101 targets because their 5′ regions contain between one and six Rim101 binding site core sequences (CCAAG (Bensen *et al*., 2004, Ramon *et al*., 2003)). Several additional sequences are overrepresented among all Rim101-dependent gene 5′ regions (1.5 Kb) in our dataset, as determined by RSAT analysis (van Helden *et al*., 1998, van Helden *et al*., 2000), including

GGTTAA, CAAGAA, and TCGTCA (see examples in Table 2). In many cases, the CAAGAA is part of a Rim101 consensus site (CCAAGAA (Bensen *et al*., 2004, Ramon *et al*., 2003)), but the other sequences may represent binding sites for Rim101-dependent transcription factors that mediate indirect regulation.

We also found 155 new Rim101-repressed genes, out of a total of 164 Rim101-repressed genes in our dataset. Ninety-one of these genes have one or more 5′ region Rim101 binding site core sequences and thus may be direct targets. The sequences AATTGC and TGAAAA are overrepresented in the repressed gene 5′ regions (see examples in Table 2), and may be binding sites for mediators of Rim101 regulation.

Role of Rim101 in OPC

Overexpression of any of five genes, *ALS3, CHT2, PGA7/RBT6, SKN1*, and *ZRT1*, partially rescued the epithelial cell interaction defects of the *rim101Δ/Δ* mutant. The extent of epithelial cell damage caused by *C. albicans* is closely related to the number of fungal cells that are endocytosed by the epithelial cells (Chiang *et al*., 2007, Park *et al*., 2005). However, our current data suggest that damage and endocytosis can be dissociated from one another because overexpression of *SKN1* restored epithelial cell damage, but not endocytosis. Conversely, overexpression of *PGA7/RBT6* and *ZRT1* partially restored endocytosis, but not cell damage. Further evidence of the dissociation between endocytosis and damage was seen with the *rim101Δ/Δ nrg1Δ/Δ+pRIM101* strain. Although this strain was endocytosed by epithelial cells more avidly than the wild-type strain, it caused less epithelial cell damage. A possible explanation for these results is that the different strains have different surface characteristics and therefore bind to different epithelial cell receptors. These disparate receptors mediate endocytosis into different intracellular compartments within the epithelial cell, which influences the extent of epithelial cell damage.

These findings argue that cell surface defects are a key component of the *rim101*Δ/Δ virulence defect, because four of the five Rim101 target genes that affect epithelial cell interactions govern cell wall features. Two of the genes that increased cell damage, *CHT2* and *SKN1*, have roles in cell wall polysaccharide structure: Cht2 is a chitinase, and Skn1 is a putative glucosidase that is implicated by homology in β-1,6-glucan synthesis (McCreath *et al*., 1996, Selvaggini *et al*., 2004, Mio *et al*., 1997). Two of the genes that enhanced endocytosis, *ALS3* and *PGA7/RBT6*, specify known or predicted GPI-linked cell surface proteins (De Groot *et al*., 2003, Phan *et al*., 2007, Hoyer *et al*., 1998). Als3 is known to function as an adhesin/invasin in several contexts (Zhao *et al*., 2004, Nobile *et al*., 2006, Phan *et al*., 2007), in keeping with the conclusion from our overexpression analysis here. Pga7/Rbt6 has not been recognized previously as a prospective invasin. It has significant similarity to several other Rim101-regulated cell wall proteins, including Rbt5, Pga10, Csa2, and Csa1 (Bensen *et al*., 2004), all of which share the cysteine-rich CFEM domain (Kulkarni *et al*., 2003). Most of these proteins are small compared to known adhesins, but Rbt5, Pga10, and Csa1 have all been implicated in biofilm adherence (Nobile *et al*., 2006, Perez *et al*., 2006). Our hypothesis is that Rim101 governs multiple cell surface features that contribute to host cell interaction both directly, as adhesins (Als3, Pga7/Rbt6), and indirectly, through cell wall modifications that may improve secretion of cell damage factors or survival after endocytosis (Cht2, Skn1).

Zrt1 is a putative low-affinity zinc transporter that is predicted to be a transmembrane protein (Braun *et al*., 2005). The effect of Zrt1 on *C. albicans* endocytosis may be indirect as zinc is required for the function of numerous enzymes and transcription factors. However, Zrt1 biological function is also connected to the cell wall, as several secretory pathway activities (protein folding, GPI anchor addition, proteolytic processing) are zinc-dependent (Eide, 2006). Thus Zrt1 overexpression may ultimately affect the same aspect of host interaction that is affected in the other TGO strains.

It was notable that *SAP5* overexpression did not cause increased epithelial cell damage in this study. Prior studies have shown that *SAP5* overexpression rescues a *rim101Δ/Δ* defect in another surrogate virulence model, an assay for invasion of reconstituted human epithelium (Villar *et al*., 2007). Villar et al. showed that Sap5 is critical for E-cadherin degradation, which in turn disrupts epithelial tissue integrity. Degradation required at least four hours of incubation with *C. albicans* in that system, whereas our epithelial cell damage assays are completed within three hours. Thus it is reasonable that different contributions to virulence would be most readily detectable in these two systems.

Virulence of *C. albicans* is thought to be multifactorial (Cutler, 1991), and it is not surprising that a transcriptional regulator like Rim101 governs several virulence mechanisms. Adhesins and secreted proteases are well recognized participants in host cell interaction (Navarro-Garcia *et al*., 2001). Our studies also point to new aspects of this interaction: the roles of small CFEM proteins and of cell wall polysaccharide. Three functionally significant target genes, *CHT2, SKN1*, and *PGA7/RBT6*, have 5′ Rim101 binding sites (Bensen *et al*., 2004, Ramon *et al*., 2003). We suggest that the effects of Rim101 on adherence and damage reflect direct roles of the Rim101 pathway in virulence.

MATERIALS AND METHODS

Construction of Fungal Strains

All *C. albicans* strains used in this study were derived from BWP17 (Wilson *et al*., 1999) and are listed in Table 1. Primer sequences from 5′ to 3′ are listed in Supplemental data, “Primer sequences” worksheet. Construction of DAY25 (*rim101Δ/Δ*) (Davis *et al*., 2000a), DAY5 (Davis *et al*., 2000b), DAY44 (*rim101Δ/Δ* +p*RIM101*) (Davis *et al*., 2000b), and DAY185 (reference strain) (Davis *et al*., 2000b) was described previously. Construction of CJN649 (*nrg1*Δ/Δ) was made by PCR-product-directed gene deletion (Wilson *et al*., 1999) with 100-mer oligonucleotides NRG1null-5DR and NRG1null-3DR via consecutive rounds of transformation into BWP17. For gene complementation, PCR was used to generate a fragment for *NRG1* from 1000 bp upstream of the start codon to 500 bp downstream of the stop codon. This fragment was inserted into the pGEMT-Easy vector (Promega), digested with NgoMIV and AlwNI, and subsequently inserted by in vivo recombination in *S. cerevisiae* into NotI- and EcoRI-digested *HIS1* vector pDDB78 (Spreghini *et al*., 2003), yielding plasmid pCJN104. The complemented strain CJN706 was made by transforming CJN649 with Nru1-digested plasmid pCJN104, directing integration to the *HIS1* locus. The *nrg1Δ/Δ* mutant strain was made His+ by transforming CJN649 with Nru1-digested pDDB78 to yield strain CJN721. Strain CJN759 (*rim101Δ/Δ nrg1*Δ/Δ double mutant) was generated via consecutive rounds of transformation into VIC18 (*rim101Δ;::dpl200/rim101Δ;::dpl200*) (Davis *et al*., 2002) using NRG1null-5DR and NRG1null-3DR oligonucleotides. CJN793, the *NRG1* complemented strain in the *rim101Δ/Δ nrg1*Δ/Δ double mutant, was made by transforming CJN759 with Nru1-digested plasmid pCJN104. CJN783, the *RIM101* complemented strain in the *rim101*Δ/Δ *nrg1*Δ/Δ double mutant, was made by transforming CJN759 with Nru1-digested plasmid pDDB61 (Davis *et al*., 2000b). CJN775, the His+ *rim101*Δ/Δ *nrg1*Δ/Δ double mutant was made by transforming CJN759 with Nru1-digested pDDB78. *C. albicans* transformants were selected for on synthetic medium (2% dextrose, 6.7% yeast nitrogen base with ammonium sulfate, and auxotrophic supplements). Genotypes were verified by colony PCR.

The *TDH3* promoter was chosen for overexpression analysis because it was found to be highly and constitutively expressed during epithelial cell damage in a previous array experiment (Filler, unpublished data). The *NAT1-TDH3* promoter plasmid pCJN542 (for gene overexpression) was generated as follows. PCR was done using primers TDH3-Fpro-SpeI and TDH3-Rpro-NdeI to generate an 800 bp product containing the *C. albicans TDH3* promoter (abbreviated *TDH3p*) with flanking NdeI and SpeI restriction sites around the promoter. This

PCR fragment was digested with NdeI and SpeI and ligated into NdeI- and SpeI-digested plasmid pCJN498 (Nobile *et al*., 2006) to create pCJN542 containing the *Ashbya gossypii TEF1* promoter (abbreviated *TEF1p*) next to the *C. albicans NAT1* ORF, followed by the *A. gossypii TEF1* terminator, followed by the *C. albicans TDH3p* in the correct orientation. The *TDH3-ZRT1* overexpression strains, CJN1364 and CJN1365, were constructed by transforming CJN793, the *NRG1* complemented strain in the *rim101*Δ/Δ *nrg1*Δ/Δ double mutant, using PCR products from template plasmid pCJN542 and primers ZRT1-F-OE-Ag-NAT-Ag-TEF1p-CJN and ZRT1-R-OE-Ag-NAT-Ag-TDH3p-CJN. These primers amplify the entire *A. gossypii TEF1p*, the *C. albicans NAT1* ORF, the *A. gossypii TEF1* terminator, and the *C. albicans TDH3p* with 100 bp of hanging homology to 500 bp upstream into the promoter of *ZRT1* for the forward primer and 100 bp of hanging homology from exactly the start codon of *ZRT1*. The homology in these primers allows for homologous recombination of the entire cassette directly upstream of the natural locus of *ZRT1* so that its expression is driven by the *TDH3p* instead of its natural promoter. By the same method, primers ECE1-F-OE-Ag-NAT-Ag-TEF1p and ECE1-R-OE-Ag-NAT-Ag-TDH3p-CJN were used for overexpression of *ECE1* to produce strains CJN1371 and CJN1372; SAP5-F-OE-Ag-NAT-Ag-TEF1p and SAP5-R-OE-Ag-NAT-Ag-TDH3p-CJN for overexpression of *SAP5* (strains CJN1379 and CJN1380); CHT2-F-OE-Ag-NAT-Ag-TEF1p and CHT2-R-OE-Ag-NAT-Ag-TDH3p-CJN for overexpression of *CHT2* (strains CJN1387 and CJN1388); SKN1-F-OE-Ag-NAT-Ag-TEF1p-CJN and SKN1-R-OE-Ag-NAT-Ag-TDH3p-CJN for overexpression of *SKN1* (strains CJN1395 and CJN1396); CSA1-F-OE-Ag-NAT-Ag-TEF1p-CJN and CSA1-R-OE-Ag-NAT-Ag-TDH3p-CJN for overexpression of *CSA1* (strains CJN1403 and CJN1404); PGA7-F-OE-Ag-NAT-Ag-TEF1p-CJN and PGA7-R-OE-Ag-NAT-Ag-TDH3p-CJN for overexpression of *PGA7/RBT6* (strains CJN1411 and CJN1412); CFL2-F-OE-Ag-NAT-Ag-TEF1p-CJN and CFL2-R-OE-Ag-NAT-Ag-TDH3p-CJN for overexpression of *CFL2* (strains CJN1419 and CJN1420); FAA2-F-OE-Ag-NAT-Ag-TEF1p-CJN and FAA2-R-OE-Ag-NAT-Ag-TDH3p-CJN for overexpression of *FAA2* (strains CJN1427 and CJN1428); and ALS3-F-OE-Ag-NAT-Ag-TEF1p and ALS3-R-OE-Ag-NAT-Ag-TDH3p for overexpression of *ALS3* (strains CJN1321 and CJN1322). Each overexpression strain was produced by an independent transformation. The transformation into *C. albicans* strains and selection on YPD+clonNAT (2% Bacto Peptone, 2% dextrose,1% yeast extract, and 400 μg/mL clonNAT (Werner BioAgents) plates was done as previously described (Nobile *et al*., 2006). Correct integration of the constructs was verified by colony PCR using a forward detection primer annealing to a sequence within the promoter of each gene of interest for each gene (Supplemental data, "Primer sequences" worksheet) in combination with the reverse primer Nat-OE-R-det2-CJN annealing to a sequence found in the *NAT* gene. Function of this overexpression strategy was verified for *ZRT1, ECE1, SAP5, CHT2*, *SKN1, CSA1, PGA7/RBT6, CFL2/FRE2*, and *FAA2* by real-time RT-PCR (Supplemental Figure 2) and for *ALS3* by flow cytometry (Supplemental Figure 3).

Media and Growth Conditions

Prior to use in the experiments, all strains were grown overnight in liquid YPD medium in a shaking incubator at 30°C. The organisms were harvested by centrifugation, washed twice in phosphate buffered saline (PBS), resuspended in RPMI 1640 medium (Irvine Scientific). They were sonicated briefly to produce singlet cells and then counted using a hemacytometer.

Hyphal induction assays were done in liquid M199 medium (Invitrogen), pH 8.0 at 37°C. To produce germ tubes, yeast form cells were incubated in RPMI 1640 medium at 37°C in a shaking incubator for 90 min for the epithelial cell damage assays or for 75 min for the flow cytometry assays. For phenotypic characterization, strains were grown overnight in YPD at 30°C, and OD_{600} values were determined. Solid media was prepared with the addition of 2% Bacto-agar. To analyze the response of the strains to lithium and alkaline pH, 5 μL of the

overnight culture was spotted onto plates of YPD, YPD + 150 mM LiCl, YPD + 150 mM HEPES buffered at pH 9.0, and M199 medium + 150 mM HEPES buffered at pH 8.2; and streaked for singles on the plate. Plates were grown at 37°C for 2 days for all assays, except M199 medium, which was grown at 37°C for 5 days.

Oral Epithelial Cells

The FaDu oral epithelial cell line, which was originally derived from a pharyngeal carcinoma, was obtained from the ATCC (ATCC Number HTB-43). The cells were grown in MEM Earl's salts (Irvine Scientific) containing 10% fetal bovine serum, 1 mM pyruvic acid, 2 mM L-glutamine, 0.1 mM non-essential amino acids, 100 IU/ml penicillin, and 100 IU/ml streptomycin. All experiments were performed using cells at 90% confluency and incubated in 5% CO_2 at 37°C.

Epithelial Cell Damage Assay

The extent of damage to epithelial cells caused by the various *C. albicans* strains was determined using a chromium release assay as described previously (Park *et al*., 2005, Martinez-Lopez *et al*., 2006, Chiang *et al*., 2007). The epithelial were grown in 96-well tissue culture plates, loaded with ^{51}Cr and infected with 10^5 organisms per well. When the overexpression strains were tested in this assay, they were added to the host cells as germ tubes because we found that there was stronger expression of the Rim101 target genes in germ tubes (data not shown). After 3 hr of incubation, the medium and cells were collected, and their respective ^{51}Cr content was measured by γ-counting. Wells containing uninfected epithelial cells were processed in parallel to determine the spontaneous release of ^{51}Cr. After correcting for well-to-well differences in the incorporation of ^{51}Cr, the percent specific release of ^{51}Cr was calculated using the following formula: (experimental release - spontaneous release)/(total incorporation - spontaneous release). Experimental release was the amount of ^{51}Cr released into the medium by epithelial cells infected with *C. albicans*. Spontaneous release was the amount of ^{51}Cr released into the medium by uninfected epithelial cells. Total incorporation was the sum of the amount of ^{51}Cr released into the medium and remaining in the epithelial cells. Each assay was performed in triplicate at least three times, and differences in epithelial cell damage caused by the various strains were evaluated by analysis of variance. *P* values of ≤ 0.05 were considered to be significant.

Microscopy

The various strains were imaged using differential interference contrast to determine their morphology while growing on FaDu oral epithelial cells. The epithelial cells were grown on 12 mm diameter glass coverslips that had been coated with fibronectin and placed in a 24-well tissue culture plate. Next, 10^5 cells of each *C. albicans* strain suspended in RPMI 1640 medium were added to different wells. After 90 min of incubation, the medium above the cells was aspirated and the cells were fixed in 3% paraformaldehyde. The coverslips were mounted inverted onto slides, after which the organisms were viewed by differential interference contrast.

Adherence and Invasion Assay—The capacity of each strain of *C. albicans* to adhere to and invade epithelial cells was measured using our previously described differential fluorescence assay (Park *et al*., 2005, Martinez-Lopez *et al*., 2006, Chiang *et al*., 2007). Briefly, 10^5 cells of each strain were added to epithelial cells that were grown on fibronectin coated glass coverslips as in the microscopy experiments. When the *rim101Δ/Δ nrg1Δ/Δ* strains were tested, the organisms were added to the epithelial cells in the state in which they grew in the YPD liquid culture, and the incubation period was 90 min. When the overexpression strains were tested, the organisms were added to the epithelial cells as germ tubes, and the incubation

period was 45 min. At the end of the incubation period, the cells were rinsed twice with Hank's balanced salt solution (HBSS; Irvine Scientific) in a standardized manner and then fixed with 3% paraformaldehyde. The adherent, but non-endocytosed organisms were labeled with rabbit polyclonal anti-*C. albicans* antibodies (Biodesign International) that had been conjugated with the red fluorescent dye, Alexa 568 (Invitrogen). Next, the cells were permeablized with 0.5% Triton X-100 (Sigma-Aldrich) in PBS, and the cell-associated organisms (the endocytosed plus non-endocytosed organisms) were labeled with anti-*C. albicans* antibodies conjugated with the green fluorescent dye, Alexa 488 (Invitrogen). The coverslips were viewed by epifluorescence and the number endocytosed organisms was determined by subtracting the number of non-endocytosed organisms (which fluoresced red) from the number of cell-associated organisms (which fluoresced green). At least 100 organisms were examined on each coverslip and the results were expressed as number of endocytosed or cell-associated organisms per high-powered field. An organism was considered to be endocytosed when all or part of it was internalized by an epithelial cell. Each assay was performed in triplicate at least three times, and differences among the various strains were evaluated by analysis of variance. *P* values of ≤ 0.05 were considered to be significant.

Mouse Model of Oropharyngeal Candidiasis

To assess the virulence of the various strains of *C. albicans*, the mouse model of OPC was used (Park *et al*., 2005, Chiang *et al*., 2007). This study was approved by the Animal Use Committee of the Los Angeles Biomedical Institute in compliance with NIH guidelines for the ethical treatment of animals. Male Balb/c mice (National Cancer Institute) weighing approximately 20 gm were immunosuppressed with cortisone acetate (Sigma-Aldrich) at a dose of 225 mg/kg administered subcutaneously on days - 1, +1 and +3 relative to the day of infection. To induce OPC, the mice were anesthetized with xylazine and ketamine (both from Phoenix pharmaceuticals) administered intraperitoneally. Next, calcium alginate urethral swabs (Type 4 Calgiswab; Puritan Medical Products Company LLC) were saturated with *C. albicans* by placing them in HBSS containing 10^6 organisms per ml. The saturated swabs were placed sublingually in the anesthetized mice for 75 min. Each strain of *C. albicans* was inoculated into 7 to 9 mice. After the mice recovered from anesthesia, they were given food and water ad libitum. The mice were sacrificed after 5 days of infection, after which their tongues and adjacent sublingual tissue were excised and then divided in half. One half was weighed, homogenized, and quantitatively cultured on Sabauroud dextrose agar containing chloramphenicol. The other half was used for histopathologic examination. The tissue was fixed in zinc-buffered formalin and embedded in paraffin for thin sectioning. The sections were stained with periodic acid-Schiff. Differences in oral fungal burden among mice infected with different strains were analyzed using the Wilcoxon rank sum test. *P* values of ≤ 0.05 were considered to be significant.

RNA Isolation and Expression Analysis

RPMI 1640 medium was inoculated with organisms from a YPD 30°C overnight culture to obtain a starting OD_{600} of 0.05 and was incubated at 37°C. Cells were harvested by vacuum filtration when the OD_{600} was 1. RNA was isolated using a hot-phenol method as previously described (Spellman *et al*., 1998) for Northern analysis, and using the RiboPure-Yeast RNA extraction kit (Ambion) as per the manufacturers instructions for microarray, RT-PCR, and real time RT-PCR analyses. Northern analysis was performed as described previously to verify the expression levels of *CHT2, ECE1*, and *RBT5* (Nobile *et al*., 2005). RT-PCR analysis was performed as described previously (Nobile *et al*., 2005) to verify the expression levels of *SAP5, SAP6*, and *ZRT1* using the primers SAP5F195 and SAP5R1075 for *SAP5*; SAP6F614 and SAP6R1197 for *SAP6*; and ZRT1FATG and ZRT1RUTR for *ZRT1* listed in Supplemental data, "Primer sequences" worksheet. Eleven 2-fold dilutions of cDNA were used for this analysis, as well as a no RT control. Flow cytometry was used to verify the surface expression

levels of *ALS3*, as previously described (Phan *et al*., 2007). For quantitative real time RT-PCR analysis, 10 μg total RNA was DNase treated at 37°C for 1 hr using the DNA-free kit (Ambion), cDNA was synthesized using the AffinityScript multiple temperature cDNA synthesis kit (Stratagene), and quantitative real time RT-PCR was done using the iQ SYBR Green Supermix (Bio-Rad) as previously described (Norice *et al*., 2007) using the primers ZRT1FATG and ZRT1RUTR for *ZRT1*; ECE1-F-qRT-CJN and ECE1-R-qRT-CJN for *ECE1*; SAP5F195 and SAP5R1075 for *SAP5*; CHT2 FWD PR and CHT2 REV PR for *CHT2*; SKN1-F-qRT-CJN and SKN1-R-qRT-CJN for *SKN1*; CSA1-F-qRT-CJN and CSA1-R-qRT-CJN for *CSA1*; PGA7F-RT-CJN and PGA7R-RT-CJN for *PGA7/RBT6*, CFL2-F-qRT-CJN and CFL2-R-qRT-CJN for *CFL2/FRE2*; and FAA2-F-qRT-CJN and FAA2-R-qRT-CJN for *FAA2* listed in Supplemental data, "Primer sequences" worksheet. In order to control for DNA contamination, reverse transcriptase was omitted from a control set of samples. Samples were processed in triplicate, and real time RT-PCR was performed using the iCycler iQ detection system (Bio-Rad) with the following program: initial denaturation at 95°C for 5 min, followed by 40 cycles of 95°C for 45 sec, 58°C for 30 sec, and 72°C for 30 sec. Amplification specificity was determined by melting curve analysis. Bio-Rad iQ5 software was used to calculate normalized gene expression values using the ΔΔCt method, using *TDH3* as a reference gene. For ease of interpretation, the reference strain expression level values were set to 1.0 for each target gene set, and the normalized expression of each gene relative to *TDH3* expression is shown in Supplemental Figure 2.

Transcriptional profiling on long oligonucleotide microarrays was performed as previously described (Nantel *et al*., 2006). We conducted four individual hybridization experiments from four pairs of independently-produced RNA samples of CJN775 versus CJN793. LOWESS normalization and statistical analysis of the data was conducted in GeneSpring GX version 7.3 (Agilent Technologies). A volcano-plot algorithm was used to identify genes that exhibited statistical significance (P values < 0.05) with a change in transcript abundance of at least 1.5-fold. The results of this analysis with adjusted P values < 0.05 are listed in the Supplemental data, "Rim101 regulated" worksheet.

Flow cytometric detection of Als3 surface expression—Flow cytometry was used to quantify the amount of Als3 expressed on the surface of the various strains. Germ tubes were produced by incubating yeast form cells of each strain in RPMI 1640 medium at 37°C for 75 min. Next, the germ tubes were fixed in 3% paraformaldehyde, blocked with 1% goat serum, and then incubated with a rabbit anti-Als3 antiserum that had been adsorbed on hyphae of an *als3Δ/Δ* mutant strain of *C. albicans* (Phan *et al*., 2007). After being rinsed extensively with PBS, the germ tubes were incubated with an Alexa 488-labeled goat anti-rabbit IgG secondary antibody. The cells were analyzed using a Becton Dickenson FACS calibur flow cytometer with gating on germ tubes with the same forward and side scatter characteristics. Ten thousand germ tubes of each strain were analyzed.

Supplementary Material

Refer to Web version on PubMed Central for supplementary material.

ACKNOWLEDGMENTS

We thank our anonymous reviewers for useful critics and comments on this manuscript. We thank all members of the Mitchell and Filler labs for comments and advice. We are indebted to Aaron Hernday for his help in analysis of the quantitative real time RT-PCR data, to Jill Blankenship, Jason Rauceo, and Carmelle Norice for providing primers and guidance for the quantitative real time RT-PCR analysis; and to Frank Smith and Jessica Hamaker for technical assistance. We also gratefully acknowledge the assistance of Hyunsook Park and Quynh T. Phan for animal experiments. We are grateful for the availability of the Candida Genome Database, without which this work would

not have been possible. This is NRC publication number 49559. This study was supported by grants 1R01DE017088 and 9R01AI070272 from the National Institutes of Health.

Abbreviations

OPC, oropharyngeal candidiasis; TGO strain, target gene overexpressing strain; PBS, phosphate buffered saline; HBSS, Hank's balanced salt solution.

REFERENCES

Arechiga-Carvajal ET, Ruiz-Herrera J. The RIM101/pacC homologue from the basidiomycete Ustilago maydis is functional in multiple pH-sensitive phenomena. Eukaryotic cell 2005;4:999–1008. [PubMed: 15947192]

Badrane H, Cheng S, Nguyen MH, Jia HY, Zhang Z, Weisner N, Clancy CJ. Candida albicans IRS4 contributes to hyphal formation and virulence after the initial stages of disseminated candidiasis. Microbiology (Reading, England) 2005;151:2923–2931.

Bensen ES, Martin SJ, Li M, Berman J, Davis DA. Transcriptional profiling in Candida albicans reveals new adaptive responses to extracellular pH and functions for Rim101p. Molecular microbiology 2004;54:1335–1351. [PubMed: 15554973]

Bignell E, Negrete-Urtasun S, Calcagno AM, Arst HN Jr. Rogers T, Haynes K. Virulence comparisons of Aspergillus nidulans mutants are confounded by the inflammatory response of p47phox-/-mice. Infection and immunity 2005;73:5204–5207. [PubMed: 16041040]

Braun BR, Kadosh D, Johnson AD. NRG1, a repressor of filamentous growth in C.albicans, is down-regulated during filament induction. The EMBO journal 2001;20:4753–4761. [PubMed: 11532939]

Braun BR, van Het Hoog M, d'Enfert C, Martchenko M, Dungan J, Kuo A, et al. A human-curated annotation of the Candida albicans genome. PLoS genetics 2005;1:36–57. [PubMed: 16103911]

Calera JA, Zhao XJ, De Bernardis F, Sheridan M, Calderone R. Avirulence of Candida albicans CaHK1 mutants in a murine model of hematogenously disseminated candidiasis. Infection and immunity 1999;67:4280–4284. [PubMed: 10417206]

Caracuel Z, Roncero MI, Espeso EA, Gonzalez-Verdejo CI, Garcia-Maceira FI, Di Pietro A. The pH signalling transcription factor PacC controls virulence in the plant pathogen Fusarium oxysporum. Molecular microbiology 2003;48:765–779. [PubMed: 12694620]

Chiang LY, Sheppard DC, Bruno VM, Mitchell AP, Edwards JE Jr. Filler SG. Candida albicans protein kinase CK2 governs virulence during oropharyngeal candidiasis. Cellular microbiology 2007;9:233–245. [PubMed: 16939537]

Cutler JE. Putative virulence factors of Candida albicans. Annual review of microbiology 1991;45:187–218.

Davis D, Edwards JE Jr. Mitchell AP, Ibrahim AS. Candida albicans RIM101 pH response pathway is required for host-pathogen interactions. Infection and immunity 2000a;68:5953–5959. [PubMed: 10992507]

Davis D, Wilson RB, Mitchell AP. RIM101-dependent and-independent pathways govern pH responses in Candida albicans. Molecular and cellular biology 2000b;20:971–978. [PubMed: 10629054]

Davis DA, Bruno VM, Loza L, Filler SG, Mitchell AP. Candida albicans Mds3p, a conserved regulator of pH responses and virulence identified through insertional mutagenesis. Genetics 2002;162:1573–1581. [PubMed: 12524333]

De Groot PW, Hellingwerf KJ, Klis FM. Genome-wide identification of fungal GPI proteins. Yeast (Chichester, England) 2003;20:781–796.

Drago L, Mombelli B, De Vecchi E, Bonaccorso C, Fassina MC, Gismondo MR. Candida albicans cellular internalization: a new pathogenic factor? International journal of antimicrobial agents 2000;16:545–547. [PubMed: 11118877]

Edmond MB, Wallace SE, McClish DK, Pfaller MA, Jones RN, Wenzel RP. Nosocomial bloodstream infections in United States hospitals: a three-year analysis. Clin Infect Dis 1999;29:239–244. [PubMed: 10476719]

Eide DJ. Zinc transporters and the cellular trafficking of zinc. Biochim Biophys Acta 2006;1763:711–722. [PubMed: 16675045]

Enoch DA, Ludlam HA, Brown NM. Invasive fungal infections: a review of epidemiology and management options. Journal of medical microbiology 2006;55:809–818. [PubMed: 16772406]

Felk A, Kretschmar M, Albrecht A, Schaller M, Beinhauer S, Nichterlein T, et al. Candida albicans hyphal formation and the expression of the Efg1-regulated proteinases Sap4 to Sap6 are required for the invasion of parenchymal organs. Infection and immunity 2002;70:3689–3700. [PubMed: 12065511]

Hoyer LL, Payne TL, Bell M, Myers AM, Scherer S. Candida albicans ALS3 and insights into the nature of the ALS gene family. Current genetics 1998;33:451–459. [PubMed: 9644209]

Kamran M, Calcagno AM, Findon H, Bignell E, Jones MD, Warn P, et al. Inactivation of transcription factor gene ACE2 in the fungal pathogen Candida glabrata results in hypervirulence. Eukaryotic cell 2004;3:546–552. [PubMed: 15075283]

Korting HC, Hube B, Oberbauer S, Januschke E, Hamm G, Albrecht A, et al. Reduced expression of the hyphal-independent Candida albicans proteinase genes SAP1 and SAP3 in the efg1 mutant is associated with attenuated virulence during infection of oral epithelium. Journal of medical microbiology 2003;52:623–632. [PubMed: 12867554]

Kulkarni RD, Kelkar HS, Dean RA. An eight-cysteine-containing CFEM domain unique to a group of fungal membrane proteins. Trends in biochemical sciences 2003;28:118–121. [PubMed: 12633989]

Lamb TM, Mitchell AP. The transcription factor Rim101p governs ion tolerance and cell differentiation by direct repression of the regulatory genes NRG1 and SMP1 in Saccharomyces cerevisiae. Molecular and cellular biology 2003;23:677–686. [PubMed: 12509465]

Lane S, Birse C, Zhou S, Matson R, Liu H. DNA array studies demonstrate convergent regulation of virulence factors by Cph1, Cph2, and Efg1 in Candida albicans. The Journal of biological chemistry 2001;276:48988–48996. [PubMed: 11595734]

Liu H. Transcriptional control of dimorphism in Candida albicans. Current opinion in microbiology 2001;4:728–735. [PubMed: 11731326]

Lo HJ, Kohler JR, DiDomenico B, Loebenberg D, Cacciapuoti A, Fink GR. Nonfilamentous C. albicans mutants are avirulent. Cell 1997;90:939–949. [PubMed: 9298905]

MacCallum DM, Findon H, Kenny CC, Butler G, Haynes K, Odds FC. Different consequences of ACE2 and SWI5 gene disruptions for virulence of pathogenic and nonpathogenic yeasts. Infection and immunity 2006;74:5244–5248. [PubMed: 16926418]

Martinez-Lopez R, Park H, Myers CL, Gil C, Filler SG. Candida albicans Ecm33p is important for normal cell wall architecture and interactions with host cells. Eukaryotic cell 2006;5:140–147. [PubMed: 16400176]

McCreath KJ, Specht CA, Liu Y, Robbins PW. Molecular cloning of a third chitinase gene (CHT1) from Candida albicans. Yeast (Chichester, England) 1996;12:501–504.

Mio T, Yamada-Okabe T, Yabe T, Nakajima T, Arisawa M, Yamada-Okabe H. Isolation of the Candida albicans homologs of Saccharomyces cerevisiae KRE6 and SKN1: expression and physiological function. Journal of bacteriology 1997;179:2363–2372. [PubMed: 9079924]

Murad AM, Leng P, Straffon M, Wishart J, Macaskill S, MacCallum D, et al. NRG1 represses yeast-hypha morphogenesis and hypha-specific gene expression in Candida albicans. The EMBO journal 2001;20:4742–4752. [PubMed: 11532938]

Nantel, A.; Rigby, T.; Hogues, H.; Whiteway, M. Medical Mycology: Cellular and Molecular Techniques. Kavanaugh, K., editor. Wiley Press; 2006.

Navarro-Garcia F, Sanchez M, Nombela C, Pla J. Virulence genes in the pathogenic yeast Candida albicans. FEMS microbiology reviews 2001;25:245–268. [PubMed: 11250036]

Nobile CJ, Andes DR, Nett JE, Smith FJ, Yue F, Phan QT, et al. Critical role of Bcr1-dependent adhesins in C. albicans biofilm formation in vitro and in vivo. PLoS pathogens 2006;2:e63. [PubMed: 16839200]

Nobile CJ, Mitchell AP. Regulation of cell-surface genes and biofilm formation by the C. albicans transcription factor Bcr1p. Curr Biol 2005;15:1150–1155. [PubMed: 15964282]

Norice CT, Smith FJ Jr. Solis N, Filler SG, Mitchell AP. Requirement for Candida albicans Sun41 in biofilm formation and virulence. Eukaryotic cell 2007;6:2046–2055. [PubMed: 17873081]

Park H, Myers CL, Sheppard DC, Phan QT, Sanchez AA, J EE, Filler SG. Role of the fungal Ras-protein kinase A pathway in governing epithelial cell interactions during oropharyngeal candidiasis. Cellular microbiology 2005;7:499–510. [PubMed: 15760450]

Penalva MA, Arst HN Jr. Recent advances in the characterization of ambient pH regulation of gene expression in filamentous fungi and yeasts. Annual review of microbiology 2004;58:425–451.

Perez A, Pedros B, Murgui A, Casanova M, Lopez-Ribot JL, Martinez JP. Biofilm formation by Candida albicans mutants for genes coding fungal proteins exhibiting the eight-cysteine-containing CFEM domain. FEMS yeast research 2006;6:1074–1084. [PubMed: 17042757]

Phan QT, Belanger PH, Filler SG. Role of hyphal formation in interactions of Candida albicans with endothelial cells. Infection and immunity 2000;68:3485–3490. [PubMed: 10816502]

Phan QT, Myers CL, Fu Y, Sheppard DC, Yeaman MR, Welch WH, et al. Als3 is a Candida albicans invasin that binds to cadherins and induces endocytosis by host cells. PLoS biology 2007;5:e64. [PubMed: 17311474]

Ramirez MA, Lorenz MC. Mutations in alternative carbon utilization pathways in Candida albicans attenuate virulence and confer pleiotropic phenotypes. Eukaryotic cell 2007;6:280–290. [PubMed: 17158734]

Ramon AM, Fonzi WA. Diverged binding specificity of Rim101p, the Candida albicans ortholog of PacC. Eukaryotic cell 2003;2:718–728. [PubMed: 12912891]

Rollins JA. The Sclerotinia sclerotiorum pac1 gene is required for sclerotial development and virulence. Mol Plant Microbe Interact 2003;16:785–795. [PubMed: 12971602]

Saville SP, Lazzell AL, Monteagudo C, Lopez-Ribot JL. Engineered control of cell morphology in vivo reveals distinct roles for yeast and filamentous forms of Candida albicans during infection. Eukaryotic cell 2003;2:1053–1060. [PubMed: 14555488]

Schaller M, Korting HC, Borelli C, Hamm G, Hube B. Candida albicans-secreted aspartic proteinases modify the epithelial cytokine response in an in vitro model of vaginal candidiasis. Infection and immunity 2005;73:2758–2765. [PubMed: 15845479]

Selvaggini S, Munro CA, Paschoud S, Sanglard D, Gow NA. Independent regulation of chitin synthase and chitinase activity in Candida albicans and Saccharomyces cerevisiae. Microbiology (Reading, England) 2004;150:921–928.

Spellman PT, Sherlock G, Zhang MQ, Iyer VR, Anders K, Eisen MB, et al. Comprehensive identification of cell cycle-regulated genes of the yeast Saccharomyces cerevisiae by microarray hybridization. Molecular biology of the cell 1998;9:3273–3297. [PubMed: 9843569]

Spreghini E, Davis DA, Subaran R, Kim M, Mitchell AP. Roles of Candida albicans Dfg5p and Dcw1p cell surface proteins in growth and hypha formation. Eukaryotic cell 2003;2:746–755. [PubMed: 12912894]

Staib P, Kretschmar M, Nichterlein T, Hof H, Morschhauser J. Transcriptional regulators Cph1p and Efg1p mediate activation of the Candida albicans virulence gene SAP5 during infection. Infection and immunity 2002;70:921–927. [PubMed: 11796627]

van Helden J, Andre B, Collado-Vides J. Extracting regulatory sites from the upstream region of yeast genes by computational analysis of oligonucleotide frequencies. Journal of molecular biology 1998;281:827–842. [PubMed: 9719638]

van Helden J, Andre B, Collado-Vides J. A web site for the computational analysis of yeast regulatory sequences. Yeast (Chichester, England) 2000;16:177–187.

Villar CC, Kashleva H, Dongari-Bagtzoglou A. Role of Candida albicans polymorphism in interactions with oral epithelial cells. Oral microbiology and immunology 2004;19:262–269. [PubMed: 15209998]

Villar CC, Kashleva H, Nobile CJ, Mitchell AP, Dongari-Bagtzoglou A. Mucosal tissue invasion by Candida albicans is associated with E-cadherin degradation, mediated by transcription factor Rim101p and protease Sap5p. Infection and immunity 2007;75:2126–2135. [PubMed: 17339363]

Wheeler RT, Fink GR. A drug-sensitive genetic network masks fungi from the immune system. PLoS pathogens 2006;2:e35. [PubMed: 16652171]

Wilson RB, Davis D, Mitchell AP. Rapid hypothesis testing with Candida albicans through gene disruption with short homology regions. Journal of bacteriology 1999;181:1868–1874. [PubMed: 10074081]

You BJ, Choquer M, Chung KR. The Colletotrichum acutatum gene encoding a putative pH-responsive transcription regulator is a key virulence determinant during fungal pathogenesis on citrus. Mol Plant Microbe Interact 2007;20:1149–1160. [PubMed: 17849717]

Zhao X, Oh SH, Cheng G, Green CB, Nuessen JA, Yeater K, et al. ALS3 and ALS8 represent a single locus that encodes a Candida albicans adhesin; functional comparisons between Als3p and Als1p. Microbiology (Reading, England) 2004;150:2415–2428.

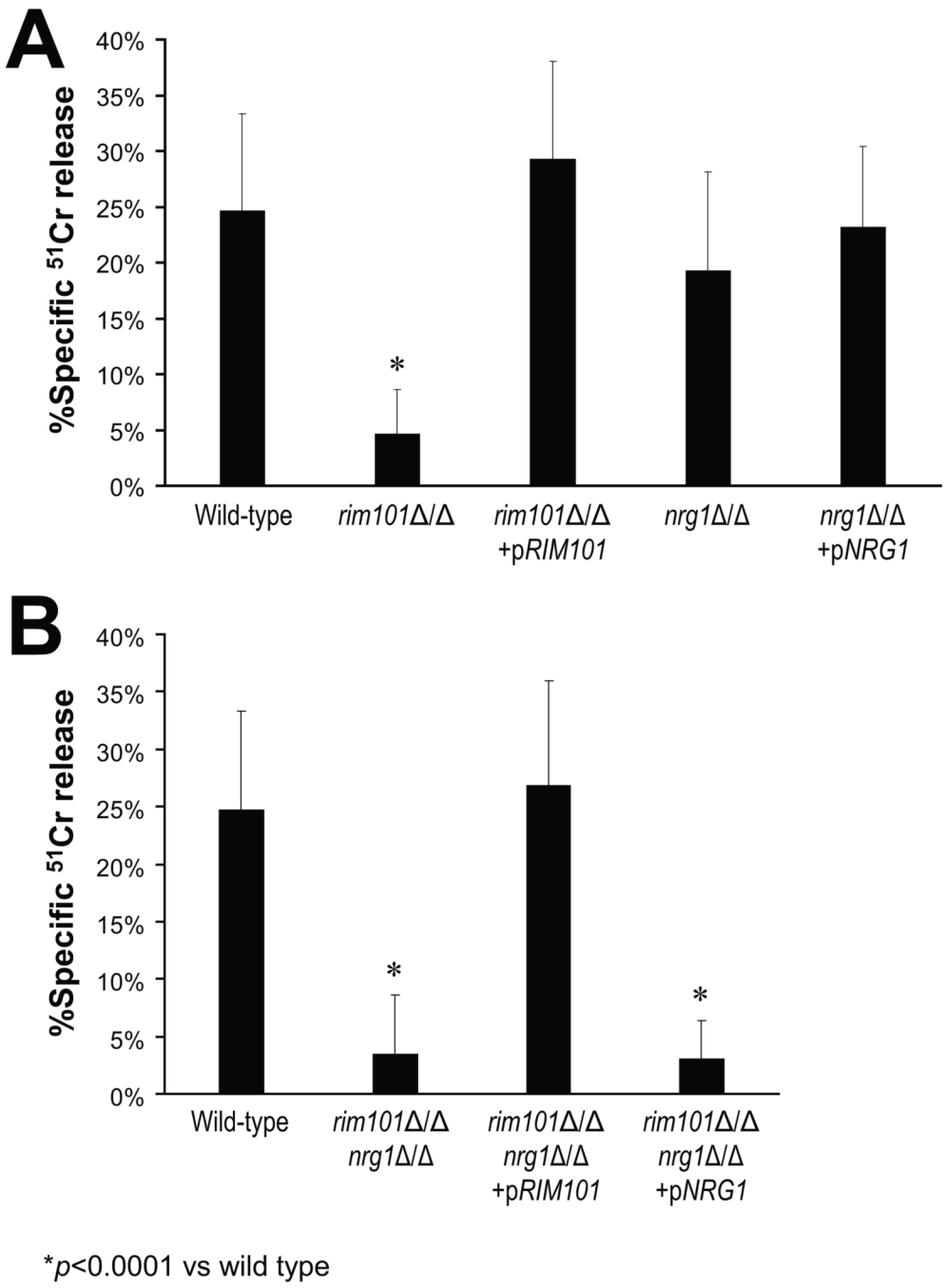

Figure 1.

Rim101 is required for *C. albicans* to damage oral epithelial cells in vitro. Single (A) or double (B) mutant strains of *C. albicans* were incubated with the FaDu oral epithelial cell line for 3 hr, after which the extent of epithelial cell injury was determined by a ^{51}Cr release assay. Results are the mean ± SD of three experiments, each performed in triplicate. *$P < 0.0001$ compared to the wild-type strain.

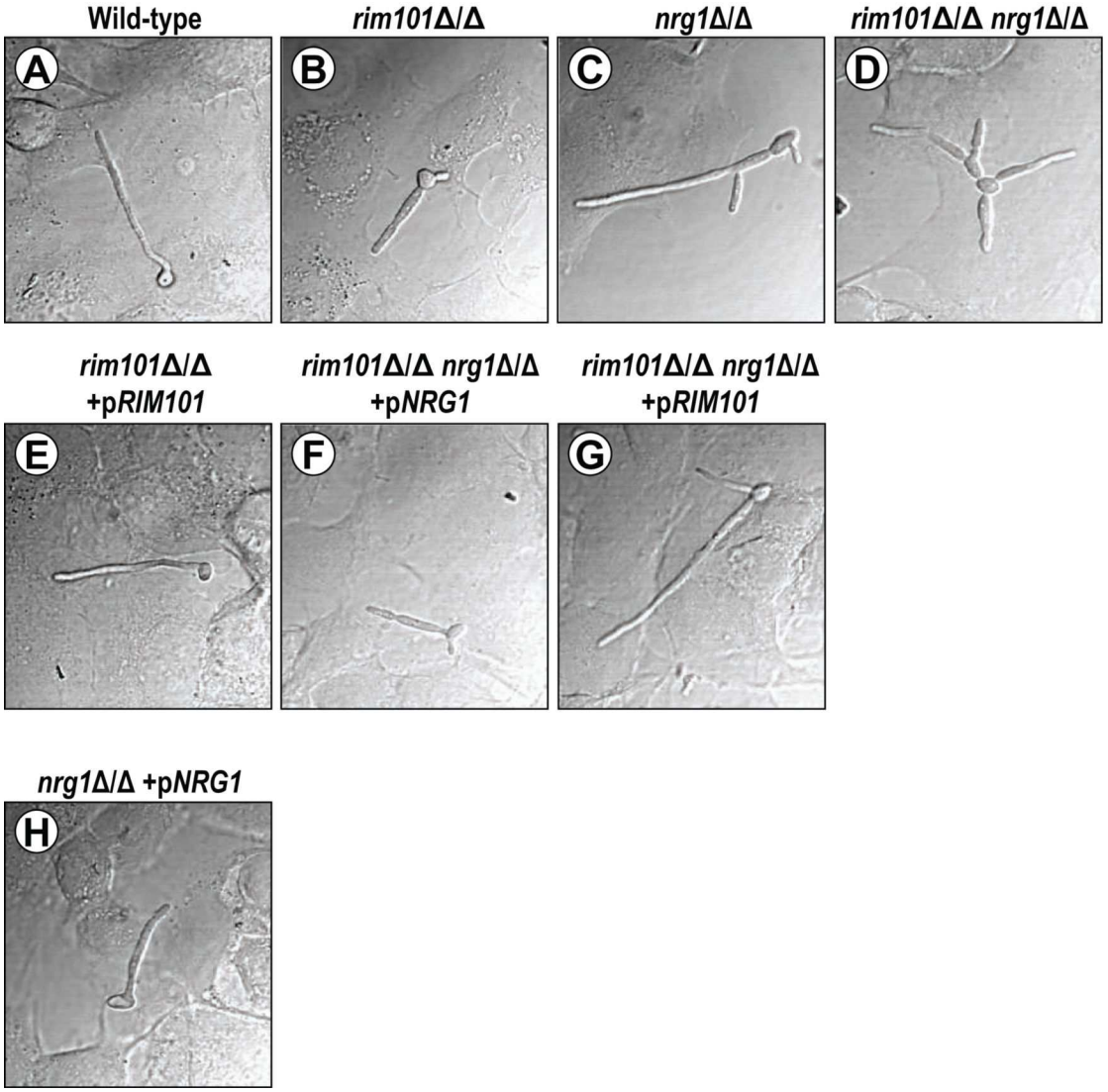

Figure 2.

Rim101 and Nrg1 influence the morphology of *C. albicans* on oral epithelial cells. Strains of *C. albicans* were incubated on FaDu oral epithelial cells for 3 hr, fixed with paraformaldehyde, and imaged using differential interference contrast microscopy. Images were taken at 1000X magnification.

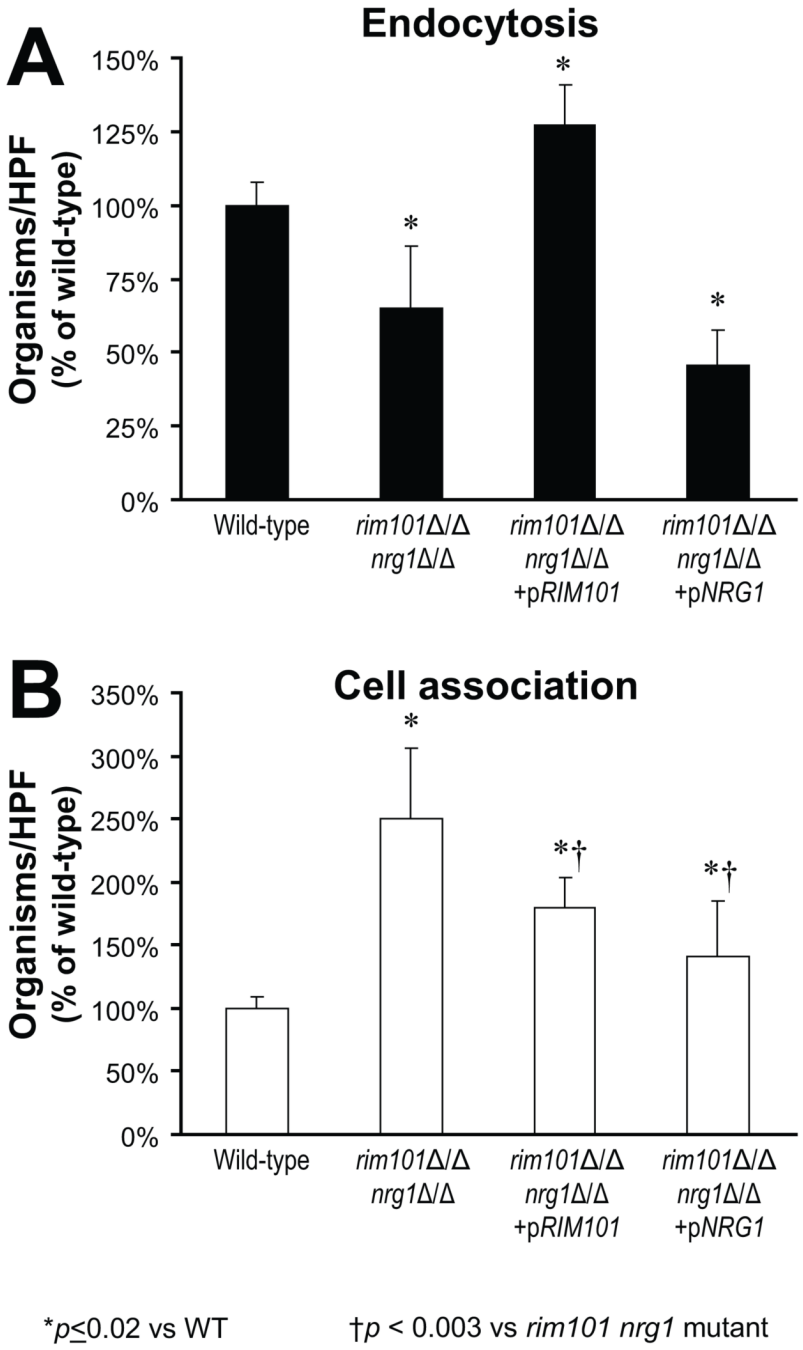

Figure 3.

Rim101 and Nrg1 govern *C. albicans* invasion and adherence to oral epithelial cells. Strains were incubated with FaDu oral epithelial cells for 90 min, after which the number of endocytosed (A) and cell-associated (B) organisms per high-powered field were determined by a differential fluorescence assay. Results of three experiments performed in triplicate are normalized to the percentage of the wild-type control strain. The endocytosis of the wild-type strains was 289 organisms per 100 high-powered fields and the mean number of cells of the wild-type strain that were associated with epithelial cells was 634 organisms per 100 high-powered fields. *$P < 0.02$ compared to the wild-type strain; $^{\dagger}p < 0.003$ compared to the *rim101*Δ/Δ *nrg1*Δ/Δ mutant.

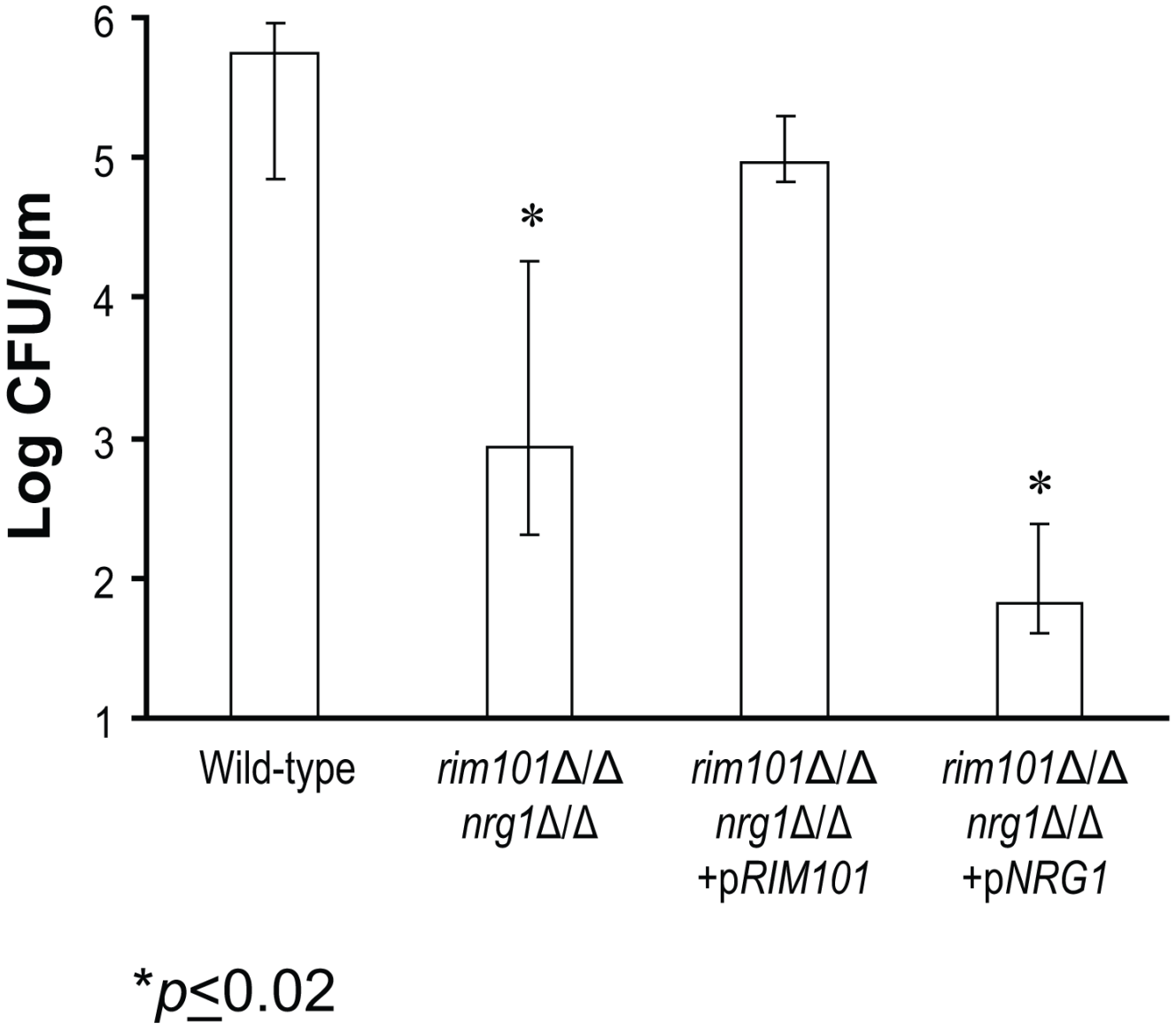

Figure 4.

Contribution of Rim101 and Nrg1 to virulence during OPC. Mice were immunosuppressed with cortisone acetate and then orally inoculated with the indicated strains (7 to 9 mice per strain). After 5 days the mice were sacrificed and oral fungal burden was determined. Results are the median ± interquartile range. *$P \leq 0.02$ compared to the wild-type strain and the *rim101*Δ/Δ *nrg1*Δ/Δ + p*RIM101* complemented strain.

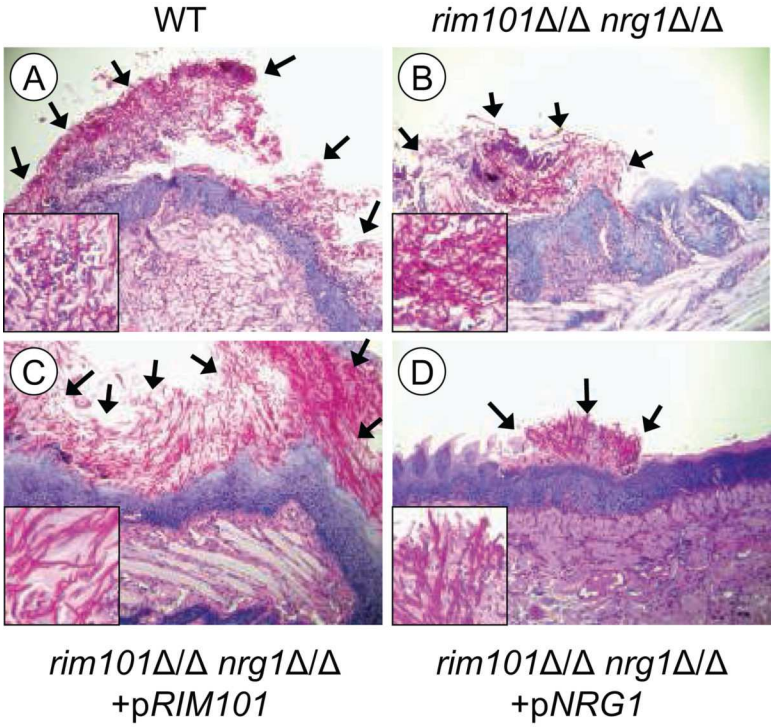

Figure 5.

Oral histopathology of mice infected with wild-type (A), *rim101*Δ/Δ *nrg1*Δ/Δ (B), *rim101*Δ/Δ *nrg1*Δ/Δ + p*RIM101* (C), and *rim101*Δ/Δ *nrg1*Δ/Δ + p*NRG1* (D) strains of *C. albicans*. Periodic acid-Schiff stained sections of the tongues of immunosuppressed mice after 5 days of infection are shown. Arrows indicate the foci of infection. The red staining areas in the lesions are the organisms. Original magnification of the large images is 100X; original magnification of the insets is 400X.

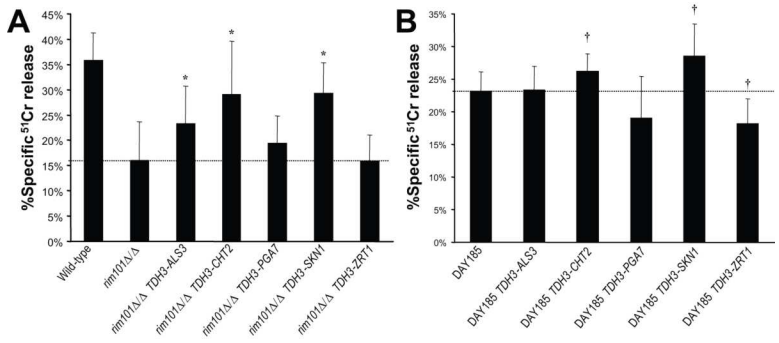

Figure 6.

Effects of overexpression of Rim101 target genes on *C. albicans* damage to oral epithelial cells. (A) Extent of FaDu oral epithelial cell damage after 3 hr infection with a wild-type strain, a *rim101*Δ/Δ mutant, or an indicated *rim101*Δ/Δ mutant TGO strain. Two independent clones of each TGO strain were tested. (B) Extent of FaDu oral epithelial cell damage after 3 h infection with a wild-type strain (DAY185) that overexpressed the indicated Rim101 target genes. Results are the mean ± SD of three experiments, each performed in triplicate. *$P < 0.02$ compared to the *rim101*Δ/Δ mutant; $^{\dagger}p < 0.04$ compared to DAY185.

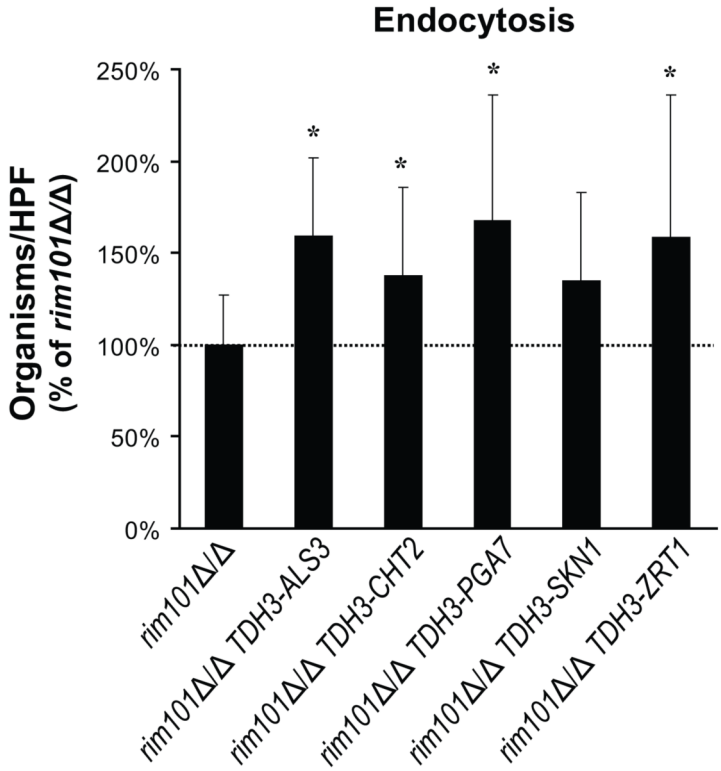

Figure 7.

Effects of overexpression of Rim101 target genes on *C. albicans* invasion of and adherence to oral epithelial cells. FaDu oral epithelial cell were infected for 45 min with a *rim101*Δ/Δ mutant, or an indicated *rim101*Δ/Δ mutant TGO strain. Two independent clones of each TGO strain were tested. The number of endocytosed organisms was determined by differential fluorescence assay. Results are normalized to the percentage of the *rim101*Δ/Δ mutant and are the mean ± SD of three experiments, each performed in triplicate. The mean endocytosis of the *rim101Δ/Δ* mutant was 28 organisms per 100 high-powered fields. **P* < 0.05 compared to the *rim101*Δ/Δ mutant.

Table 1

C. albicans strains

Strain	Genotype	Reference
CJN649	$\frac{ura3\Delta::\lambda imm434}{ura3\Delta::\lambda imm434}\ \frac{arg4::hisG}{arg4::hisG}\ \frac{his1::hisG}{his1::hisG}\ \frac{nrg1::ARG4}{nrg1::URA3}$	This Study
CJN706	$\frac{ura3\Delta::\lambda imm434}{ura3\Delta::\lambda imm434}\ \frac{arg4::hisG}{arg4::hisG}\ \frac{his1::hisG::pHIS1-NRG1}{his1::hisG}\ \frac{nrg1::ARG4}{nrg1::URA3}$	This Study
CJN721	$\frac{ura3\Delta::\lambda imm434}{ura3\Delta::\lambda imm434}\ \frac{arg4::hisG}{arg4::hisG}\ \frac{his1::hisG::pHIS1}{his1::hisG}\ \frac{nrg1::ARG4}{nrg1::URA3}$	This Study
CJN759	$\frac{ura3\Delta::\lambda imm434}{ura3\Delta::\lambda imm434}\ \frac{arg4::hisG}{arg4::hisG}\ \frac{his1::hisG}{his1::hisG}\ \frac{rim101::dpl200}{rim101::dpl200}\ \frac{nrg1::ARG4}{nrg1::URA3}$	(Villar *et al.*, 2007)
CJN775	$\frac{ura3\Delta::\lambda imm434}{ura3\Delta::\lambda imm434}\ \frac{arg4::hisG}{arg4::hisG}\ \frac{his1::hisG::pHIS1-}{his1::his}\ \frac{rim101::dpl200}{rim101::dpl200}\ \frac{nrg1::ARG4}{nrg1::URA3}$	This Study
CJN783	$\frac{ura3\Delta::\lambda imm434}{ura3\Delta::\lambda imm434}\ \frac{arg4::hisG}{arg4::hisG}\ \frac{his1::hisG}{his1::hisG}\ \frac{rim101::dpl200}{rim101::dpl200}\ \frac{nrg1::ARG4}{nrg1::URA3}\ \frac{pRIM101::His1}{RIM101}$	This Study
CJN793	$\frac{ura3\Delta::\lambda imm434}{ura3\Delta::\lambda imm434}\ \frac{arg4::hisG}{arg4::hisG}\ \frac{his1::hisG::pHIS1-NRG1}{his1::hisG}\ \frac{rim101::dpl200}{rim101::dpl200}\ \frac{nrg1::ARG4}{nrg1::URA3}$	(Villar *et al.*, 2007)
CJN1321 and CJN1322	$\frac{ura3\Delta::\lambda imm434\,arg4::hisG}{ura3\Delta::\lambda imm434\,arg4::hisG}\ \frac{his1::hisG::pHIS1-NRG1}{his1::hisG}\ \frac{rim101::dpl200}{rim101::dpl200}\ \frac{nrg1::ARG4}{nrg1::URA3}\ \frac{ALS3::pAgTEF1-NAT1-AgTEF1UTR-TDH3\,ALS3}{ALS3}$	This Study
CJN1330	$\frac{ura3\Delta::\lambda imm434}{ura3\Delta::\lambda imm434}\ \frac{ARG4::URA3::arg4::hisG}{arg4::hisG}\ \frac{his1::hisG::pHIS1}{his1::hisG}\ \frac{ALS3::pAgTEF1-NAT1-AgTEF1UTR-TDH3-ALS3}{ALS3}$	This Study
CJN1364 and CJN1365	$\frac{ura3\Delta::\lambda imm434\,arg4::hisG}{ura3\Delta::\lambda imm434\,arg4::hisG}\ \frac{his1::hisG::pHIS1-NRG1}{his1::hisG}\ \frac{rim101::dpl200}{rim101::dpl200}\ \frac{nrg1::ARG4}{nrg1::URA3}\ \frac{ZRT1::pAgTEF1-NAT1-AgTEF1UTR-TDH3-ZRT1}{ZRT}_1$	This Study
CJN1371 and CJN1372	$\frac{ura3\Delta::\lambda imm434\,arg4::hisG}{ura3\Delta::\lambda imm434\,arg4::hisG}\ \frac{his1::hisG::pHIS1-NRG1}{his1::hisG}\ \frac{rim101::dpl200}{rim101::dpl200}\ \frac{nrg1::ARG4}{nrg1::URA3}\ \frac{ECE1::pAgTEF1-NAT1-AgTEF1UTR-TDH3-ECE1}{ECE1}$	This Study
CJN1379 and CJN1380	$\frac{ura3\Delta::\lambda imm434\,arg4::hisG}{ura3\Delta::\lambda imm434\,arg4::hisG}\ \frac{his1::hisG::pHIS1-NRG1}{his1::hisG}\ \frac{rim101::dpl200}{rim101::dpl200}\ \frac{nrg1::ARG4}{nrg1::URA3}\ \frac{SAP5::pAgTEF1-NAT1-AgTEF-1UTR-TDH3-SAP5}{SAP5}$	This Study
CJN1387 and CJN1388	$\frac{ura3\Delta::\lambda imm434\,arg4::hisG}{ura3\Delta::\lambda imm434\,arg4::hisG}\ \frac{his1::hisG::pHIS1-NRG1}{his1::hisG}\ \frac{rim101::dpl200}{rim101::dpl200}\ \frac{nrg1::ARG4}{nrg1::URA3}\ \frac{CHT2::pAgTEF1-NAT1-AgTEF1UTR-TDH3-CHT2}{CHT2}$	This Study
CJN1395 and CJN1396	$\frac{ura3\Delta::\lambda imm434\,arg4::hisG}{ura3\Delta::\lambda imm434\,arg4::hisG}\ \frac{his1::hisG::pHIS1-NRG1}{his1::hisG}\ \frac{rim101::dpl200}{rim101::dpl200}\ \frac{nrg1::ARG4}{nrg1::URA3}\ \frac{SKN1::pAgTEF1-NAT1-AgTEF1UTR-TDH3-SKN1}{SKN1}$	This Study
CJN1403 and CJN1404	$\frac{ura3\Delta::\lambda imm434\,arg4::hisG}{ura3\Delta::\lambda imm434\,arg4::hisG}\ \frac{his1::hisG::pHIS1-NRG1}{his1::hisG}\ \frac{rim101::dpl200}{rim101::dpl200}\ \frac{nrg1::ARG4}{nrg1::URA3}\ \frac{CSA1::pAgTEF1-NAT1-AgTEF1UTR-TDH3-CSA1}{CSA1}$	This Study
CJN1411 and CJN1412	$\frac{ura3\Delta::\lambda imm434\,arg4::hisG}{ura3\Delta::\lambda imm434\,arg4::hisG}\ \frac{his1::hisG::pHIS1-NRG1}{his1::hisG}\ \frac{rim101::dpl200}{rim101::dpl200}\ \frac{nrg1::ARG4}{nrg1::URA3}\ \frac{PGA7::pAgTEF1-NAT1-AgTEF1UTR-TDH3-PGA7}{PGA7}$	This Study
CJN1419 and CJN1420	$\frac{ura3\Delta::\lambda imm434\,arg4::hisG}{ura3\Delta::\lambda imm434\,arg4::hisG}\ \frac{his1::hisG::pHIS1-NRG1}{his1::hisG}\ \frac{rim101::dpl200}{rim101::dpl200}\ \frac{nrg1::ARG4}{nrg1::URA3}\ \frac{CFL2::pAgTEF1-NAT1-AgTEF1UTR-TDH3-CFL2}{CFL2}$	This Study
CJN1427 and CJN1428	$\frac{ura3\Delta::\lambda imm434\,arg4::hisG}{ura3\Delta::\lambda imm434\,arg4::hisG}\ \frac{his1::hisG::pHIS1-NRG1}{his1::hisG}\ \frac{rim101::dpl200}{rim101::dpl200}\ \frac{nrg1::ARG4}{nrg1::URA3}\ \frac{FAA2::pAgTEF1-NAT1-AgTEF1UTR-TDH3-FAA2}{FAA2}$	This Study
CJN1580	$\frac{ura3\Delta::\lambda imm434}{ura3\Delta::\lambda imm434}\ \frac{ARG4:URA3::arg4::hisG}{arg4::hisG}\ \frac{his1::hisG::pHIS1}{his1::hisG}\ \frac{CHT2::pAgTEF1-NAT1-AgTEF1UTR-TDH3-CHT2}{CHT2}$	This Study

Strain	Genotype	Reference
CJN1587	$\frac{ura3\Delta::\lambda imm434\ ARG4:URA3::arg4::hisG\ his1::hisG::pHIS1\ ZRT1::pAgTEF-1NAT1-AgTEF\UTR-TDH3-ZRT1}{ura3\Delta::\lambda imm434\ arg4::hisG\ his1::hisG\ ZRT1}$	This Study
CJN1591	$\frac{ura3\Delta::\lambda imm434\ ARG4:URA3::arg4::hisG\ his1::hisG::pHIS1\ ECE1::pAgTEF1-NAT1-AgTEF\UTR-TDH3-ECE1}{ura3\Delta::\lambda imm434\ arg4::hisG\ his1::hisG\ ECE1}$	This Study
CJN1594	$\frac{ura3\Delta::\lambda imm434\ ARG4:URA3::arg4::hisG\ his1::hisG::pHIS1\ SAP5::pAgTEF1-NAT1-AgTEF\UTR-TDH3-SAP5}{ura3\Delta::\lambda imm434\ arg4::hisG\ his1::hisG\ SAP5}$	This Study
CJN1597	$\frac{ura3\Delta::\lambda imm434\ ARG4:URA3::arg4::hisG\ his1::hisG::pHIS1\ PGA7::pAgTEF1-NAT1-AgTEF\UTR-TDH3-PGA7}{ura3\Delta::\lambda imm434\ arg4::hisG\ his1::hisG\ PGA7}$	This Study
CJN1601	$\frac{ura3\Delta::\lambda imm434\ ARG4:URA3::arg4::hisG\ his1::hisG::pHIS1\ CSA1::pAgTEF1-NAT1-AgTEF\UTR-TDH3-CSA1}{ura3\Delta::\lambda imm434\ arg4::hisG\ his1::hisG\ CSA1}$	This Study
CJN1605	$\frac{ura3\Delta::\lambda imm434\ ARG4:URA3::arg4::hisG\ his1::hisG::pHIS1\ SKN1::pAgTEF1-NAT1-AgTEF\UTR-TDH3-SKN1}{ura3\Delta::\lambda imm434\ arg4::hisG\ his1::hisG\ SKN1}$	This Study
CJN1609	$\frac{ura3\Delta::\lambda imm434\ ARG4:URA3::arg4::hisG\ his1::hisG::pHIS1\ CFL2::pAgTEF1-NAT1-AgTEF\UTR-TDH3-CFL2}{ura3\Delta::\lambda imm434\ arg4::hisG\ his1::hisG\ CFL2}$	This study
CJN1613	$\frac{ura3\Delta::\lambda imm434\ ARG4:URA3::arg4::hisG\ his1::hisG::pHIS1\ FAA2::pAgTEF1-NAT1-AgTEF\UTR-TDH3-FAA2}{ura3\Delta::\lambda imm434\ arg4::hisG\ his1::hisG\ FAA2}$	This Study
DAY25	$\frac{ura3\Delta::\lambda imm434\ arg4::hisG\ his1::hisG::pHIS1\ rim101::ARG4}{ura3\Delta::\lambda imm434\ arg4::hisG\ his1::hisG\ rim101::URA3}$	(Davis *et al.*, 2000a)
DAY44	$\frac{ura3\Delta::\lambda imm434\ arg4::hisG\ his1::hisG::pHIS1-RIM101\ rim101::ARG4}{ura3\Delta::\lambda imm434\ arg4::hisG\ his1::hisG\ rim101::URA}$	(Davis *et al.*, 2000b)
DAY185	$\frac{ura3\Delta::\lambda imm434\ ARG4::URA3::arg4::hisG\ his1::hisG::pHIS1}{ura3\Delta::\lambda imm434\ arg4::hisG\ his1::hisG}$	(Davis *et al.*, 2000a)
VIC18	$\frac{ura3\Delta::\lambda imm434\ arg4::hisG\ his1::hisG\ rim101::dpl200}{ura3\Delta::\lambda imm434\ arg4::hisG\ his1::hisG\ rim101::dpl200}$	(Davis *et al.*, 2002)

Table 2

Selected Rim101-regulated genes from microarray analysis

Systematic name	rim101 nrg1 vs nrg1 (log ratio)	Common name	Known or New[a]	TGO[b]	Description	Category[c]	Possible 5′ regulatory sequence[d]					
							CCAAG	AATTGC	CAAGAA	GGTTAA	TCGTCA	TGAAAA
orf19.2060	-4.94	*SOD5*	New		copper-zinc superoxide dismutase	cell wall	2	2	5			9
orf19.3829	-4.02	*PHR1*	Known		pH regulated GPI-linked protein	cell wall	3	1	4	1		3
orf19.3895	-4	*CHT2*	New	Yes	chitinase 2 precursor	cell wall	5	2	3		1	5
orf19.3117	-3.88	*CSA2*	New		mycelial surface antigen; similar to RBT5	cell wall*	1	1				1
orf19.5635	-3.55	*PGA7/RBT6*	Known	Yes	GPI-linked protein; similar to RBT5	cell wall*	2		1	1		2
orf19.3374	-3.07	*ECE1*	Known	Yes	secreted cell elongation protein	cell surface*	1	4	4	1	1	3
orf19.7114	-2.75	*CSA1*	Known	Yes	mycelial surface antigen	cell wall	4		3	1		2
orf19.5585	-2.45	*SAP5*	New	Yes	secreted aspartyl proteinase	cell surface*	3	3	2			3
orf19.7362	-2.01	*SKN1*	New	Yes	glucan synthase subunit	cell wall biogenesis	4	2	9			3
orf19.1816	-1.27	*ALS3*	New	Yes	agglutinin-like protein	cell wall	2	3	2	2		1
orf19.4211	-3.09	*FET3*	New		high-affinity iron uptake	transport	3		2	1		5
orf19.4546	-3	*HOL4*	Known		MFS multidrug-resistance protein	transport	4		2	2	2	2
orf19.4527	-2.85	*HGT1*	New		hexose transporter	transport	3		3		1	5
orf19.1264	-2.32	*CFL2/FRE2*	New	Yes	ferric reductase	transport	4	4	5	1	1	5
orf19.6070	-1.98	*ENA5*	New		Na+ ATPase	transport	3	3	3	2		4
orf19.6897	-1.54	*FET3*	New		hypothetical protein	transport	4	2				3
orf19.701	-1.2	*FRE8*	New		ferric reductase	transport	1	1	3	2		2
orf19.3112	-0.39	*ZRT1*	Known	Yes	high affinity zinc transporter	transport	3		1	3		
orf19.4076	0.99	*MET10*	New		sulfite reductase flavin-binding subunit	amino acid synthesis	2		1	1		3
orf19.1706	1.07	*MET18*	New		TFIIH regulator	amino acid synthesis				1		1
orf19.4506	1.08	*LYS22*	New		homocitrate synthase	amino acid synthesis		3	1			4
orf19.6086	1.13	*LEU4*	New		2-isopropylmalalate synthase	amino acid synthesis			1			1
orf19.7080	1.2	*LEU2*	New		isopropyl malate dehydrogenase	amino acid synthesis						2
orf19.946	1.23	*MET14*	New		adenylylsulfate kinase	amino acid synthesis	1	2		1		3
orf19.5025	2.31	*MET3*	New		ATP sulfurylase	amino acid synthesis	7	3	2	1		4

[a] Known Rim101-regulated genes had been identified previously (Bensen *et al*., 2004); new genes had not.

[b] TGO (Target Gene Overexpression) strains have been constructed for these genes.

[c] Categories represent GO function or process terms associated with each gene at the Candida Genome Database http://www.candidagenome.org/. Terms marked with an asterisk were not associated GO terms but were inferred by homology.

[d] Number of occurrences of each putative regulatory sequence in 1.5 Kb of 5′ noncoding region, as determined by RSAT analysis http://rsat.ulb.ac.be/rsat/ excluding regions of overlap with neighboring ORFs.